LncRNA HCP5 Encoding Protein Regulates Ferroptosis To Promote The Progression of Triple Negative Breast Cancer

Xiao Tong
Southeast University Medical College
Jiani Xing
Southeast University Medical College
Haizhou Liu
Nanjing University of Aeronautics and Astronautics
Shunheng Zhou
Nanjing University of Aeronautics and Astronautics
Yue Huang
Nanjing University of Aeronautics and Astronautics
Jing Lin
Institute of Cancer Prevention and Treatment
Zhengling Yu
Southeast University Medical College
Wei Jiang
Nanjing University of Aeronautics and Astronautics
Lihong Wang (lw2247@yeah.net)
Medical college of Southeast University https://orcid.org/0000-0002-6715-2944

Research article

Keywords: LncRNA HCP5, Encoding protein, Ferroptosis, ROS, Triple-negative breast cancer

Posted Date: August 3rd, 2021

DOI: https://doi.org/10.21203/rs.3.rs-746373/v1

Abstract

Background

Long non-coding RNAs (lncRNAs) is widely described as a class of RNA longer than 200 nucleotides without encoding capability. But recent years, more and more open reading frames (ORFs) have been found in lncRNAs which indicate they have coding capacity. But the mechanisms of the encoding products in cancer are mostly unknown. We have previously shown lncRNA HCP5 is an oncogene in triple negative breast cancer (TNBC), and the aim of the current study was to investigate if lncRNA HCP5 encoding protein promotes TNBC by regulating ferroptosis.

Methods

We use bioinformatics to predict coding capacity. Molecular biology experiments and the xenograft assay in nude mice to study the mechanism of lncRNA HCP5 encoding protein. And the protein expression was evaluated in a tissue microarray of 140 invasive breast tumors and 45 pared precancerous breast tissues. Association between the protein expression and clinicopathologic features of breast cancer patients was analyzed.

Results

In this study, we identify that ORF in lncRNA HCP5 can encode a conserved protein with 132-amino acid. The protein, which is named HCP5-132aa, promotes TNBC growth. Mechanistically, the HCP5-132aa regulates GPX4 expression and lipid ROS level through ferroptosis pathway to promote TNBC progression. HCP5-132aa ORF knockdown synergizes with ferroptosis activators in vitro and in vivo. Breast cancer patients with high levels of HCP5-132aa have poorer prognosis.

Conclusions

Our study indicates that overexpression of lncRNA HCP5 encoding protein is a critical oncogenic event in TNBC. Our findings uncover a regulatory mechanism of ferroptosis in TNBC orchestrated by a protein encoded by an lncRNA.

Introduction

A new report shows that the most commonly-diagnosed cancers worldwide were female breast cancer (about 2.26 million cases) [1]. In China, the incidence of breast cancer also ranks the first among female malignant tumors. Triple negative breast cancer (TNBC), which accounts for 10%-17%, is characterized by high aggressiveness and poor prognosis due to the lack of therapeutic targets [2]. However, the underlying molecular mechanisms responsible for TNBC tumorigenesis are still not fully understood.

Ferroptosis is a kind of programmed cell death, which leads to the shrinkage of mitochondria, the increase of membrane density and the decrease or disappearance of mitochondrial cristae in cell morphology [3]. This process is characterized by lipid peroxide accumulation, membrane repair and iron-dependent accumulation of reactive oxygen species (ROS) [4, 5]. Several genes and pathways responsible for the regulation of iron and ROS metabolism have been implicated in ferroptosis, such as the Xc^-/GSH/GPX4, ACSL4/LPCAT3/15-LOX and FSP1/CoQ10 pathway [6–8].

LncRNAs are widely found in organs and systems of the body [9–11]. Although once considered as the "noise" in the human genome, with the development of bioinformatics, 2% of lncRNAs have been found to encode proteins or peptides [12]. Studies had shown that tumor-related lncRNA coding proteins or peptides can be combined with traditional anticancer drugs or chemoradiotherapy to improve the therapeutic effect of cancers and reduce mortality [13]. For example, lncRNA coding peptide ASRPS involved in malignant progression of TNBC and HOXB-AS3 coding peptide inhibited the growth of CRC [14, 15]. Also a 73aa peptide encoded by CircPPP1R12A can help colon cancer metastasize [16].

In this study, we discovered that the lncRNA HLA complex P5 (HCP5), which was previously reported as an oncogene in TNBC [17], encoded a conserved 132-amino acid small protein which named HCP5-132aa. Knockdown HCP5 ORF caused low HCP5-132aa expression, induced ferroptosis by decreasing GPX4 and increasing lipid ROS in TNBC cells. High levels of the HCP5-132aa protein were associated with a poor survival rate in breast cancer patients. Collectively, we revealed that a protein encoded by lncRNA HCP5 promoted the malignant progression of TNBC through inhibiting ferroptosis.

Material And Methods

Prediction of lncRNA HCP5 encoding products using bioinformatics analysis

To identify the lncRNA HCP5 encoded peptides or proteins in breast cancer, we integratively analyzed HCP5 open reading frame (ORF), ribosome profile (Ribo-seq) and MS/MS data of MDA-MB-231 cell line (Fig. S1). LncRNA HCP5 sequence (GRCh38 fasta format) was obtained from NCBI Gene [18]. Ribo-seq data (GSE69923) and MS/MS data (PXD008222) were downloaded from Gene Expression Omnibus (GEO) database [19] and EMBI-EBI-PRIDE database [20], respectively.

HCP5 ORFs were identified by ORFfinder [21] in NCBI based on HCP5 exon sequence. We screened ORFs with start codon “ATG” in the positive strand as candidates. Then, we obtained Ribo-seq files of SRA format and converted them to fastq format by using fastq-dump tool (https://ncbi.github.io/sra-tools/fastq-dump.html). Next, adaptor sequences were trimmed using Trim Golare (https://www.bioinformatics.babraham.ac.uk/projects/trim_galore/). Reads shorter than 25 bp after adaptor trimming were discarded. rRNA sequences were filtered by using RNAcentral database [22]. Furthermore, the remaining reads were aligned to reference genome GRCh38 using TopHat2 [23] and bam format file was obtained. The ORFs fewer than 400 nt with reads mapped were regarded as convinced

HCP5 small ORFs (sORFs). In addition, MS/MS raw data was converted to mgf format by MSConvert [24]. Then, Peppy was used to get amino acid (aa) sequences for peptides or proteins and aligned to GRCh38. Finally, the convinced HCP5 sORFs with MS/MS peptides mapped were validated as highly convinced HCP5 sORFs.

Tissue samples

Breast tumor tissue microarrays (TMA) were obtained from Shanghai Outdo Biotech Co. (Shanghai, China). The TMA HBre-Duc140Sur-01 contains 140 cases of invasive ductal carcinomas and 45 pared precancerous breast tissues from the regions around cancers. No patients received adjuvant radiotherapy, chemotherapy, or immunotherapy before surgery. The experimental protocols were approved by The Human Research Ethics Committee from Medical College of Southeast University.

Immunohistochemistry staining (IHC)

The tissue sections were dried at 60°C for 1 h then dewaxed in xylene and rehydrated through graded alcohol concentrations using standard procedures. Antigen retrieval was performed in citrate buffer (pH 6.0) and autoclave at 121°C for 90 s. After washing in PBS (3 min × 3), sections were blocked with goat serum (Boster, Wuhan, China) in the room temperature for 30 min. Then each section was treated with HCP5-132aa mouse polyclonal antibodies (B01, Abnova, Inc.; at a dilution of 1:200 solution) at 4°C overnight. After washing in PBS (5 min × 3), each section was incubated with Polink-1 HRP DAB Detection System One-step polymer detection system for mouse antibody (ZSGB-BIO, Beijing, China) at room temperature for 20 min. After washing in PBS (3 min × 3), the slides were counterstained with hematoxylin. For negative controls, the primary antibody was substituted with PBS.

Reagents and cell viability assay

Ferrostatin-1 (Fer-1; SML0583) was obtained from Sigma-Aldrich, Liproxstatin-1 (Lip-1; S7699), RLS3 (S8155), Sulfasalazine (SULF; S1576) and Erastin (S7242) was obtained from Selleck. cn. MDA-MB-231 cells (5×10^4/mL) were seeded in 96-wells plates with 100 μL per well for 24 hs, then 0.099 μM, 0.197 μM, 0.375 μM, 0.625 μM, 1.25 μM, 2.5 μM, 5 μM, 10 μM and 20 μM RLS3, Sulfasalazine and Erastin were added in to plates. After 16 h, 24 h and 48 h, 10 μL of the Cell Counting Kit-8 (CCK-8) reagent was added into each well and incubated in 37°C, 5% CO_2 for 2 hours. Then cell growth was detected and calculated the inhibition rate.

Cell culture and lentivirus-mediated transduction of shRNA

Human breast cancer cell lines MDA-MB-231 and MDA-MB-468 cell lines were cultured in L-15 medium with 10% fetal bovine serum (FBS), in 37°C incubator without CO_2.

The procedure of lentivirus infection is as follows: the plate containing cells was added with appropriate amount of lentivirus in concentration gradient, followed by adding 1/1000 polybrene to enhance infection. The sequence of the HCP5-132aa shRNA was showed in Table S1. Lentivirus vector LV5

containing full-length HCP5-132aa or empty vector were purchased from GenePharma Co., Ltd. (Shanghai, China).

Cell proliferation assays

MDA-MB-231 cells and MDA-MB-468 cells were seeded in 96-wells plates and transfected with HCP5-132aa, Vector, HCP5-132aa shRNA and NCs, respectively. After transfection for 48 hours, 10 μL of the CCK-8 reagent was added into each well, incubated in 37°C, 5% CO_2 for 2 hour, and cell growth was detected by an enzyme labeling instrument at 450 nm.

Colony formation assays

For colony formation assays with monolayer culture, MDA-MB-231 cells (0.4×10^3/well) and MDA-MB-468 cells (0.4×10^3 /well) were plated in a 6-wells plates for two weeks. After fixed with methanol, the cells were stained with 0.1% crystal violet 30 min and then the colonies were imaged and counted.

Transwell

For transwell migration, 1×10^5 /ml cells were suspended in 200 μl medium without bovine serum albumin into upper chamber of 24-well transwell plates (8 μm pore size; Corning), and 500 μl of medium containing 10% FBS was added to the lower chambers. After 24 h co-culture, the cells on the lower surface of membrane were fixed in 4% paraformaldehyde, stained by 0.1% crystal violet. The stained cells were then counted under light microscope. Photographs of random fields across three replicate wells by 200 times magnification were captured for analysis.

RNA extraction and quantitative reverse transcription PCR

TRIzol (Invitrogen, USA) was used to isolate the total RNA of tissues, and cDNA was synthesi-zed with PrimeScriptTM RT Master Mix (Takara Biomedical Technology Co., Ltd, Beijing, China). A qTOWER2.0 Real-Time PCR System (Analytik Jena AG) with ChamQ Universal SYBR qPCR Master Mix (Vazyme Biotech Co., Ltd, Nanjing, China) was used to perform quantitative PCR (qPCR). Relative mRNA expression was standardized using the housekeeping GAPDH. The following human primers purchased from Sangon Biotech. (Shanghai, China) were as follows: HCP5-132aa R: 5'-GAGGCATGGCTGCTGTCACAC-3', F: 5'- TGGCTGGACGATTCTCCTCACAC-3'; GAPDH R: 5'-TCTCGCTCCTGGAAGATGGTGAT-3', F: 5'- CGGAGTCAACGGATTTGGTCG-3'. The procedures were performed in triplicate.

Western blot

MDA-MB-231 and MDA-MB-468 cells transfected with vector, HCP5-132aa, shHCP5-132aa or shNC were harvested and lysed with cell lysis buffer for western blotting (Beyotime, Shanghai, China). The proteins (30 μg per lane) were separated on 12% SDS-polyacrylamide gels and transferred into polyvinylidene fluoride (PVDF) membranes (Millipore, Billerica, MA, USA). Primary antibodies for mouse-anti-AMID/AIFM2 (B-6) (1:500) (sc-377120, Santa cruze, Inc.), mouse-anti-FTH1 (1:500) (sc-376594, Santa cruze, Inc.), mouse-anti-ACSL4 (1:500) (sc-365230, Santa cruze, Inc.), rabbit-anti-GPX4 (1:1000)

(ab125066, Abcam, USA); HCP5-132aa (1:1500) (Huabio, China) and rabbit-anti-β-actin (1:1000) (Bioss Antibodies, 10 Inc.) were incubated at 4°C overnight. Binding of the primary antibody was detected using an enhanced chemiluminescence kit (ECL Amersham). The Image J software was used to quantify and analyze each specific western blot band.

Lipid ROS assays

Lipid ROS levels were determined using C11-BODIPY dye (D3861, ThermoFisher Scientific) according to the manufacturer's instructions. Cells were seeded in six-wells plates overnight, then the culture medium was replaced with Erastin (15 μM), RSL3 (1.25 μM), Liproxstatin-1 (50 μM) or Ferrostatin-1 (1 μM) treatment for 48h. Then the medium was replaced with 5μM C11-BODIPY-containing medium for 1 h. Later, the cells were harvested by trypsin and washed three times with ice-cold PBS followed by re-suspending in PBS plus 1% BSA. The amount of ROS within cells was examined by flow cytometry analysis (FACSCantoTM II, BD Biosciences).

Iron assays

For the iron assay, we used an Iron Assay Kit (MAK025-1KT, Sigma Aldrich) to measure Fe^{2+} or total iron in each cell line. First, 2×10^6 of cells was rapidly homogenized in 4 ~ 10 volumes of Iron Assay buffer. Samples were centrifuged at 13,000 × g for 10min at 4°C to remove insoluble material. To measure ferrous iron, 5 μl of iron assay buffer was added to each well. Samples were mixed well using a horizontal shaker or by pipetting and the reactions were incubated for 30 min at room temperature in dark conditions. Then, 100 μL of Iron Probe was added to each well containing standard or test samples. Samples were mixed well using a horizontal shaker or by pipetting and the reactions were incubated for 60 min at room temperature in dark conditions. Finally, the absorbance was measured at 593 nm (A593).

Immunofluorescence analysis

Cells were fixed in 4% formaldehyde for 30 min at room temperature before cell permeabilization with 0.1% Triton X-100 (4°C, 10 min). Cells were saturated with PBS containing 2% bovine serum albumin for 1 h at room temperature and processed for immunofluorescence with 1mg/ml C11-BODIPY followed by 10mg/ml Hoechst 33258 (Invitrogen, Carlsbad, CA, USA). Between all incubation steps, cells were washed three times for 3 min with PBS containing 0.2% bovine serum albumin. Fluorescence signals were analyzed using an Olympus Fluoview 1000 confocal microscope (Olympus Corp, Tokyo, Japan).

Transmission electron microscopy (TEM)

Cells were collected and fixed in 2.5% glutaraldehyde for at least 3 h. Then the cells were treated with 2% paraformaldehyde at room temperature for 60 min and 0.1% glutaraldehyde in 0.1 M sodium cacodylate for 2 h, followed by post-fixing with 1% OsO4 for 1.5 h. After a second washing, cells were dehydrated with graded acetone and finally embedded in Quetol 812. Ultrathin sections were observed under an H7500 electron microscope (Hitachi, Tokyo, Japan).

Xenograft assay in Nude mice

For each experiment, 24 mice were randomly divided into the following four groups: (1) control shRNA model receiving DMSO (vehicle); (2) control shRNA model receiving Erastin; (3) HCP5-132aa shRNA model receiving DMSO (vehicle) and (4) HCP5-132aa shRNA model receiving Erastin. Indicated subcutaneously injected into the dorsal flanks right of the midline in nude mice (female, 4 ~ 6 weeks). At day seven, mice were intraperitoneal injected with Erastin (50 mg/kg i.v., two times a week) for three weeks. Erastin was dissolved in the vehicle (2% DMSO and 98% PBS) and prepared by Ultrasonic Cleaner (Fisher Scienti c, Hampton, NH). A final volume of 300 μL of Erastin was applied via intraperitoneal injection. And 16 mice were randomly divided into the following two groups: (1) HCP5-132aa shRNA model receiving DMSO (vehicle) and (2) HCP5-132aa shRNA model receiving RSL3. At day seven, mice were intraperitoneal injected with RSL3 (100 mg/kg i.v., two times a week) for three weeks. RSL3 was dissolved in the vehicle (2% DMSO, 2% Tween80, 30% PEG300 and 66% PBS) and prepared by Ultrasonic Cleaner (Fisher Scienti c, Hampton, NH). A final volume of 200 μL of RLS3 was applied via intraperitoneal injection. Tumors were measured twice a week. The volumes were calculated using the following formula: volume (mm^3) = length × $width^2$ × π/6.

Statistical analysis

All statistical analyses were performed using SPSS 19.0 software (IBM Corp, Armonk, NY, USA). Results are expressed as the mean ± standard deviation (SD). Group means were compared using Student's t-test for independent data. All *P*-values are two-tailed, and $P < 0.05$ was considered to indicate statistical significance. The chi-square test was used to compare HCP5-132aa expression between breast cancer tissues and paired breast tissues and the association with clinicopathologic parameters. Survival analyses were estimated using the Kaplan–Meier method.

Results

LncRNA HCP5 encoded a protein and upregulated in TNBC cell lines

HCP5 was originally annotated as an lncRNA gene located in chr6 (p21.33) in Homo sapiens and we previously reported lncRNA HCP5 promoted TNBC progression [17]. Here, we predicted that there are five convinced HCP5 sORFs with Ribo-seq reads mapped identified in exon by ORFfinder. After mapped with MS/MS peptides, three highly convinced HCP5 sORFs were remained in the following analysis (Fig. S2). The peptides encoded by HCP5 sORFs were named as small peptides (sPEPs). The lengths of identified sPEPs were 132aa, 43aa and 22aa. The sequences were shown in the Table S2. We further identified a 399bp ORF with the potential to encode a highly conserved 132aa protein which was named HCP5-132aa (Fig. 1A-C).

To determine whether HCP5-132aa was endogenously expressed, we produced antibody against the HCP5-132aa and detected via western blot analysis in MCF-10A and breast cancer cell lines. The results showed that HCP5-132aa protein expression was higher in TNBC cell lines (MDA-MB-231, MDA-MB-468

and HCC-1937 cells) than other cell lines (Fig. 1D). Next we did protein subcellular localization and we found HCP5-132aa expressed both in nucleus and cytoplasm (Fig. 1E).

HCP5-132aa high expression indicates a poor prognosis for breast cancer patients

To examine the role of the HCP5-132aa in breast cancer patients, protein levels in tissue microarray analysis of 140 pairs of breast cancer tissues and matched precancerous tissues were analyzed by IHC assay. HCP5-132aa levels increased in the TNBC tissues compared with those in the non-TNBC and precancerous tissues (Fig. 1F, Table S3 and S4, $P = 0.042$ and $P < 0.001$, respectively). Increased HCP5-132aa levels were positively associated with more advanced clinical stages of breast cancer ($P = 0.002$; Table S3). Kaplan-Meier survival analyses revealed that patients with higher HCP5-132aa levels were at increased risk of breast cancer related death compared with patients with lower HCP5-132aa expression levels (Fig. 1G-H, $P < 0.001$, log-rank test). Therefore, increased HCP5-132aa levels were correlated with a poor prognosis in breast cancer patients.

Knockdown of HCP5-132aa inhibited TNBC cell malignant phenotypes

To determine whether HCP5-132aa had a function in TNBC, HCP5-132aa ORF expression was knockdown or overexpressed in MDA-MB-231 and MDA-MB-468 cells (Fig. S3A-D). Knockdown HCP5-132aa ORF expression inhibited TNBC cell growth, colony formation, migration and promoted apoptosis (Fig. 2A-D). Also, HCP5-132aa ORF knockdown could make cell cycle arrested in S stage. The proportion of cells at G2/M phase was not changed (Fig. 2E). These results demonstrated that the HCP5-132aa is a positive regulator of TNBC progression.

HCP5-132aa knockdown promoted ferroptosis

In order to verify the regulatory mechanism of HCP5-132aa in TNBC, RNA sequencing was performed to search for the differentially expressed genes (DEGs) after HCP5-132aa ORF knockdown. We applied DEseq2 for differential expression analysis and identified 720 DEGs ($q < 0.05$ and $|\log2 (\text{Fold Change})| > \log2(1.5)$) (Fig. 3A). Then, we performed functional enrichment analysis for the DEGs by clusterProfiler R package. The result demonstrated that the DEGs were significantly enriched in 39 pathways ($P < 0.05$), which included the ferroptosis pathway (Fig. 3B).

Furthermore, we chose ferroptosis activators Erastin and RSL3 to induce ferroptosis since sulfasalazine didn't work in MDA-MB-231 cells (Fig. S4). Mitochondrial morphological changes in MDA-MB-231 were observed using TEM. After specifically knocking down HCP5-132aa ORF, the mitochondrial membrane density was increased and the mitochondrial crest was reduced, and the mitochondria damage worse when adding Erastin. But there was no obviously change of mitochondria morphology when overexpressed HCP5-132aa in the same dose Erastin stimulating MDA-MB-231 cells (Fig. 3C).

Ferroptosis can cause lipid reactive oxygen species (ROS) accumulation, we measured the lipid ROS by C11-BODIPY staining through flowcytometry and confocal after HCP5-132aa ORF knockdown and stimulating with ferroptosis stimulator or inhibitor. The results validated that the lipid ROS level increased in HCP5-132aa ORF knockdown cells and getting much higher after Erastin or RSL3-induced. Like Fer-1 and Lip-1, co-treatment with HCP5-132aa overexpression plasmid suppressed lipid ROS level in response to Erastin or RSL3 (Fig. 3D-F). But there was no significant difference in iron levels between these groups (Fig. S5A-B). Thus, we inferred that HCP5-132aa ORF downregulation could promote ferroptosis through inducing lipid ROS production.

Western blot showed that the GPX4 protein expression was reduced after knockdown of HCP5-132aa ORF or stimulated with ferroptosis activators Erastin and RLS3 compared with the control group in MDA-MB-231 and MDA-MB-468 cells. But there was no difference of other ferroptosis associated protein ACSL4, AMID and FTH between the control and HCP5-132aa knockdown groups. Ferroptosis inhibitors Fer-1 and Lip-1 could not reverse GPX4 level in MDA-MB-231, but the GPX4 protein expression could be reversed by Fer-1 in Erastin stimulated and Lip-1 in RLS3 induced HCP5-132aa knockdown MDA-MB-468 cells (Fig. 3G-J). These results indicate that knockdown HCP5-132aa ORF specifically regulates GPX4 and induced ferroptosis in TNBC cells.

HCP5-132aa knockdown synergized with ferroptosis activators inhibiting tumor growth in vivo

To assess the effect of HCP5-132aa on TNBC in vivo, we treated subcutaneous xenograft tumor of silencing HCP5-132aa ORF in nude mice with Erastin or RSL3. As shown in Fig. 4A-C, HCP5-132aa ORF knockdown inhibited tumor growth in vivo. Erastin or RSL3 inhibited the growth of tumor cells in the knockdown groups significantly. The differences in tumor weight among these groups were significant. Hematoxylin and eosin (HE) stained tissue sections showed that there were no damages in the organs (lungs, livers, kidneys and hearts) at the given dose (Fig. S6). The reduction of tumor cells was more obvious in the shRNA HCP5-132aa group and Erastin treatment groups than shNC group (Fig. 4D). These data suggested that HCP5-132aa downregulation could synergize with ferroptosis activators to inhibit tumor growth in vivo. We draw the schematic diagram of lncRNA HCP5 encoding protein HCP5-132aa induced ferroptosis through regulating GPX4 and ROS (Fig. 4E).

Discussion

Studies had shown that the expression of lncRNA HCP5 was up-regulated in glioma, cervical cancer and follicular thyroid cancer [25–27], and decreased in ovarian cancer [28]. Our previous publication indicated lncRNA HCP5 promotes TNBC progression as a ceRNA to regulate BIRC3 by sponging miR-219a-5p [17]. In this study, we provided the first evidence that lncRNA HCP5 encoding a 132aa protein, which we named HCP5-132aa. This protein can promote the malignant progression of TNBC through regulating the ferroptosis pathway in vitro and in vivo. Mechanistically, these effects are dependent on GPX4 and lipid ROS levels, no other ferroptosis associated pathways. The HCP5-132aa levels were increased in TNBC

cell lines and primary cancer tissues compared with those in their corresponding parental cell lines and precancerous tissues, respectively. Moreover, the HCP5-132aa high expression was associated with poorer patient prognoses which indicated that HCP5-132aa might have the potential to be a prognostic factor for TNBC.

Recent advances in bioinformatics and biochemical methodologies have revealed that lncRNAs may harbor concealed peptides or proteins; however, only a few have been functionally verified and characterized [16], and fewer articles reported lncRNA-encoded proteins/peptides function in cancer progression (8–9)[29]. Here, we have identified and characterized the functions of a conserved protein encoded by the lncRNA HCP5 during tumorigenesis. HCP5-132aa promotes TNBC cell growth, colony formation, migration and induced S phase cell cycle arrested. Besides, it can suppress cell apoptosis. These results indicate that HCP5-132aa is a tumor promotor.

Moreover, RNA sequencing results between the control and HCP5-132aa ORF knockdown cells suggested that the DEGs could be enriched in the ferroptosis pathway. The ferroptosis was recently discovered as an apoptosis-independent form of programmed necrosis [30]. It is characterized by the iron-dependent lethal accumulation of lipid ROS. The ferroptotic cells exhibit smaller mitochondria, diminished or vanished of mitochondria crista, and condensed mitochondrial membrane densities [6]. We verified that HCP5-132aa ORF knockdown alone could induce cell ferroptosis, suggesting that it might act as a driver of ferroptosis. So far, we are the first to propose that the protein encoded by lncRNA can promote the development of cancer through regulating ferroptosis. We found that knocking down HCP5-132aa ORF increased the mitochondrial membrane density, reduced the mitochondrial crest, and even worse when adding Erastin. But HCP5-132aa ORF overexpression could suppress the morphological changes of mitochondria induced by Erastin. We also demonstrated that HCP5-132aa knockdown could directly decrease GPX4 expression and increase ROS level. GPX4 is the only peroxidase known to efficiently reduce esterified, hydroperoxy fatty acids into unreactive alcohols. We speculated HCP5-132aa could be a GPX4 activator to promote the antioxidant response, decreasing natural lipid ROS species to accumulate. Recently, ferroptosis suppressor protein 1 (FSP1), also known as AMID, was identified as a second ferroptosis suppression mechanism through its recycling of coenzyme Q10, a radical-trapping antioxidant [31]. But the results showed other ferroptosis pathway proteins ACSL4, AMID and FTH expression were unchanged. The xenograft results suggested that knockdown HCP5-132aa ORF could synergize with ferroptosis activators to inhibit tumor growth in vivo.

Conclusions

In summary, we found that the lncRNA HCP5 encodes a protein HCP5-132aa. The HCP5-132aa promoted TNBC growth by regulating GPX4 and subsequent inhibited ROS level, thereby suppressing ferroptosis. TNBC patients with HCP5-132aa high expression exhibit more aggressive clinicopathological features and poorer prognoses. Thus, our findings expand the understanding of the pathways that regulate ferroptosis and provide an approach for exploiting ferroptosis therapeutically.

Abbreviations

LncRNA
Long non-coding RNA; ORF:open reading frames; TNBC:Triple negative breast cancer; ROS:Reactive oxygen species; HCP5:HLA complex P5; aa:amino acid; TMA:Tumor tissue microarrays; IHC:Immunohistochemistry staining.

Declarations

Ethics approval and consent to participate

Breast tumor tissue microarrays (TMA) were obtained from Shanghai Outdo Biotech Co. (Shanghai, China) and have been performed in accordance with the Declaration of Helsinki. The experimental protocols were approved by The Human Research Ethics Committee from Medical College of Southeast University.

Consent for publication

Not applicable.

Availability of data and materials

The datasets generated during and/or analysed during the present study are not publicly available, owing to confidentiality reasons, but anonymised versions may be available from the corresponding author on reasonable request.

Competing interests

The authors declare that they have no competing interests.

Funding

This work was supported by grants from the Fundamental Research Funds for the Central Universities (Grant No. 2242020K40131) and the National Natural Science Foundation of China (Grant No. 81972478 and 61872183).

Authors' contributions

LW and WJ designed the study, drafted the manuscript and obtained funding for the Generations Study. XT, and JX did molecular biology experiments and the xenograft assay in nude mice. HL, SZ and YH collected and prepared data for the analysis. JL and ZY conducted IHC experiment and cell culture. All authors contributed to data interpretation and preparation of the final manuscript. All authors read and approved the final manuscript.

Acknowledgements

We thank Department of Pharmacology in Medical School and Institute of Cancer Prevention and Treatment of Heilongjiang Academy of Medical Science for support of the Study.

References

1. Ferlay J, Colombet M, Soerjomataram I, Parkin DM, Pineros M, Znaor A, Bray F. **Cancer statistics for the year 2020: An overview**. *Int J Cancer* 2021.
2. Jemal A, Siegel R, Ward E, Hao Y, Xu J, Thun MJ. Cancer statistics, 2009. Cancer J Clin. 2009;59(4):225–49.
3. Dixon SJ, Lemberg KM, Lamprecht MR, Skouta R, Zaitsev EM, Gleason CE, Patel DN, Bauer AJ, Cantley AM, Yang WS, et al. Ferroptosis: an iron-dependent form of nonapoptotic cell death. Cell. 2012;149(5):1060–72.
4. Stockwell BR, Friedmann Angeli JP, Bayir H, Bush AI, Conrad M, Dixon SJ, Fulda S, Gascon S, Hatzios SK, Kagan VE, et al. Ferroptosis: A Regulated Cell Death Nexus Linking Metabolism, Redox Biology, and Disease. Cell. 2017;171(2):273–85.
5. Xie Y, Hou W, Song X, Yu Y, Huang J, Sun X, Kang R, Tang D. Ferroptosis: process and function. Cell death differentiation. 2016;23(3):369–79.
6. Li D, Li Y. The interaction between ferroptosis and lipid metabolism in cancer. Signal Transduct Target Ther. 2020;5(1):108.
7. Louandre C, Marcq I, Bouhlal H, Lachaier E, Godin C, Saidak Z, Francois C, Chatelain D, Debuysscher V, Barbare JC, et al. The retinoblastoma (Rb) protein regulates ferroptosis induced by sorafenib in human hepatocellular carcinoma cells. Cancer letters. 2015;356(2 Pt B):971–7.
8. Wu J, Minikes AM, Gao M, Bian H, Li Y, Stockwell BR, Chen ZN, Jiang X. Intercellular interaction dictates cancer cell ferroptosis via NF2-YAP signalling. Nature. 2019;572(7769):402–6.
9. Hu X, Sood AK, Dang CV, Zhang L. The role of long noncoding RNAs in cancer: the dark matter matters. Curr Opin Genet Dev. 2018;48:8–15.
10. Kung JT, Colognori D, Lee JT. Long noncoding RNAs: past, present, and future. Genetics. 2013;193(3):651–69.
11. Sun T. Long noncoding RNAs act as regulators of autophagy in cancer. Pharmacological research. 2018;129:151–5.
12. Zhu S, Wang J, He Y, Meng N, Yan GR. Peptides/Proteins Encoded by Non-coding RNA: A Novel Resource Bank for Drug Targets and Biomarkers. Front Pharmacol. 2018;9:1295.
13. Wu P, Mo Y, Peng M, Tang T, Zhong Y, Deng X, Xiong F, Guo C, Wu X, Li Y, et al. Emerging role of tumor-related functional peptides encoded by lncRNA and circRNA. Mol Cancer. 2020;19(1):22.
14. Wang Y, Wu S, Zhu X, Zhang L, Deng J, Li F, Guo B, Zhang S, Wu R, Zhang Z, et al: **LncRNA-encoded polypeptide ASRPS inhibits triple-negative breast cancer angiogenesis**. *The Journal of experimental*

medicine 2020, 217(3).

15. Huang JZ, Chen M, Chen, Gao XC, Zhu S, Huang H, Hu M, Zhu H, Yan GR. A Peptide Encoded by a Putative lncRNA HOXB-AS3 Suppresses Colon Cancer Growth. Molecular cell. 2017;68(1):171–84 e176.
16. Xing J, Liu H, Jiang W, Wang L. LncRNA-Encoded Peptide: Functions and Predicting Methods. Frontiers in oncology. 2020;10:622294.
17. Wang L, Luan T, Zhou S, Lin J, Yang Y, Liu W, Tong X, Jiang W: **LncRNA HCP5 promotes triple negative breast cancer progression as a ceRNA to regulate BIRC3 by sponging miR-219a-5p**. *Cancer medicine* 2019, **8**(9):4389–4403.
18. Morel A, O'Carroll AM, Brownstein MJ, Lolait SJ. Molecular cloning and expression of a rat V1a arginine vasopressin receptor. Nature. 1992;356(6369):523–6.
19. Barrett T, Wilhite SE, Ledoux P, Evangelista C, Kim IF, Tomashevsky M, Marshall KA, Phillippy KH, Sherman PM, Holko M, et al. NCBI GEO: archive for functional genomics data sets–update. Nucleic acids research. 2013;41(Database issue):D991–5.
20. Vizcaino JA, Csordas A, del-Toro N, Dianes JA, Griss J, Lavidas I, Mayer G, Perez-Riverol Y, Reisinger F, Ternent T, et al. 2016 update of the PRIDE database and its related tools. Nucleic acids research. 2016;44(D1):D447–56.
21. Sayers EW, Barrett T, Benson DA, Bolton E, Bryant SH, Canese K, Chetvernin V, Church DM, DiCuccio M, Federhen S, et al. Database resources of the National Center for Biotechnology Information. Nucleic acids research. 2011;39(Database issue):D38–51.
22. The RC. RNAcentral: a hub of information for non-coding RNA sequences. Nucleic acids research. 2019;47(D1):D221–9.
23. Kim D, Pertea G, Trapnell C, Pimentel H, Kelley R, Salzberg SL. TopHat2: accurate alignment of transcriptomes in the presence of insertions, deletions and gene fusions. Genome biology. 2013;14(4):R36.
24. Adusumilli R, Mallick P. Data Conversion with ProteoWizard msConvert. Methods in molecular biology. 2017;1550:339–68.
25. Teng H, Wang P, Xue Y, Liu X, Ma J, Cai H, Xi Z, Li Z, Liu Y. Role of HCP5-miR-139-RUNX1 Feedback Loop in Regulating Malignant Behavior of Glioma Cells. Molecular therapy: the journal of the American Society of Gene Therapy. 2016;24(10):1806–22.
26. Yu Y, Shen HM, Fang DM, Meng QJ, Xin YH: **LncRNA HCP5 promotes the development of cervical cancer by regulating MACC1 via suppression of microRNA-15a**. *European review for medical and pharmacological sciences* 2018, **22**(15):4812–4819.
27. Liang L, Xu J, Wang M, Xu G, Zhang N, Wang G, Zhao Y. LncRNA HCP5 promotes follicular thyroid carcinoma progression via miRNAs sponge. Cell death disease. 2018;9(3):372.
28. Liu N, Zhang R, Zhao X, Su J, Bian X, Ni J, Yue Y, Cai Y, Jin J. A potential diagnostic marker for ovarian cancer: Involvement of the histone acetyltransferase, human males absent on the first. Oncology letters. 2013;6(2):393–400.

29. Xiang X, Fu Y, Zhao K, Miao R, Zhang X, Ma X, Liu C, Zhang N, Qu K: **Cellular senescence in hepatocellular carcinoma induced by a long non-coding RNA-encoded peptide PINT87aa by blocking FOXM1-mediated PHB2**. *Theranostics* 2021, **11**(10):4929–4944.
30. Shaw AT, Winslow MM, Magendantz M, Ouyang C, Dowdle J, Subramanian A, Lewis TA, Maglathin RL, Tolliday N, Jacks T. Selective killing of K-ras mutant cancer cells by small molecule inducers of oxidative stress. Proc Natl Acad Sci USA. 2011;108(21):8773–8.
31. Bersuker K, Hendricks JM, Li Z, Magtanong L, Ford B, Tang PH, Roberts MA, Tong B, Maimone TJ, Zoncu R, et al. The CoQ oxidoreductase FSP1 acts parallel to GPX4 to inhibit ferroptosis. Nature. 2019;575(7784):688–92.

Figures

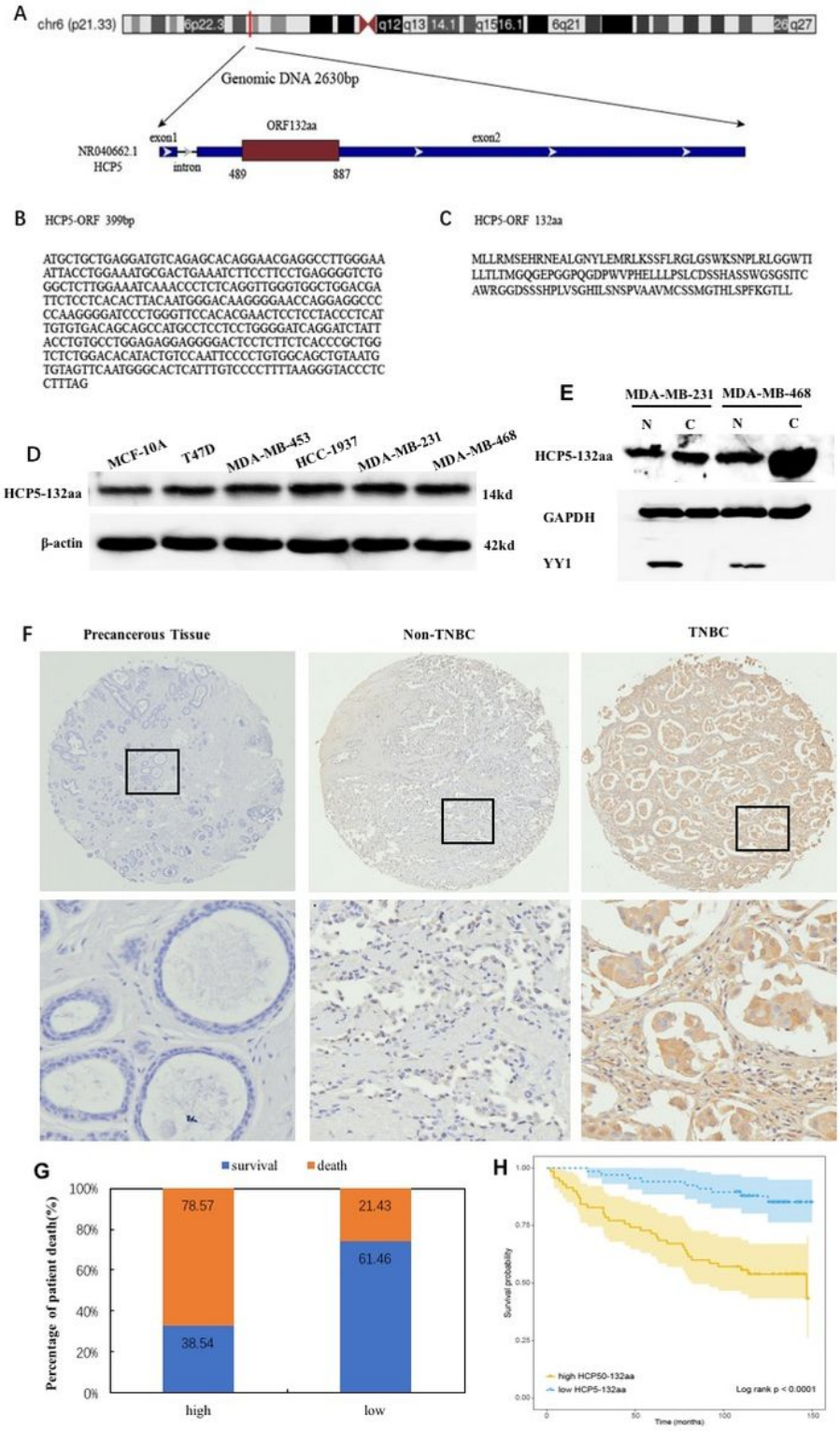

Figure 1

LncRNA HCP5 encoded a protein and endogenously up-regulated in TNBC cell lines and tissues. (A) The sketch map of lncRNA HCP5 location. (B) The ORF sequence of HCP5. (C) The 132-amino acid translated by HCP5-ORF. (D) Western blot demonstrating that HCP5-132aa was endogenously expressed in MCF-10A and breast cancer cell lines and higher in TNBC cell lines. Single representative Western blot is shown from three separate experiments. (E) Subcellular localization showed HCP5-132aa expressed both

in nucleus and cytoplasm. (F) Representative IHC images of HCP5-132aa protein expression in breast cancer tissues and their corresponding precancerous tissues (n = 140). (G) Associations between HCP5-132aa protein levels and the percentage of patient death were analyzed in breast cancer samples. (H) A Kaplan-Meier curves for overall survival of breast cancer patients with expression of HCP5-132aa. The breast cancer patients with high expression of HCP5-132aa showed worse overall survival rates (P < 0.0001).

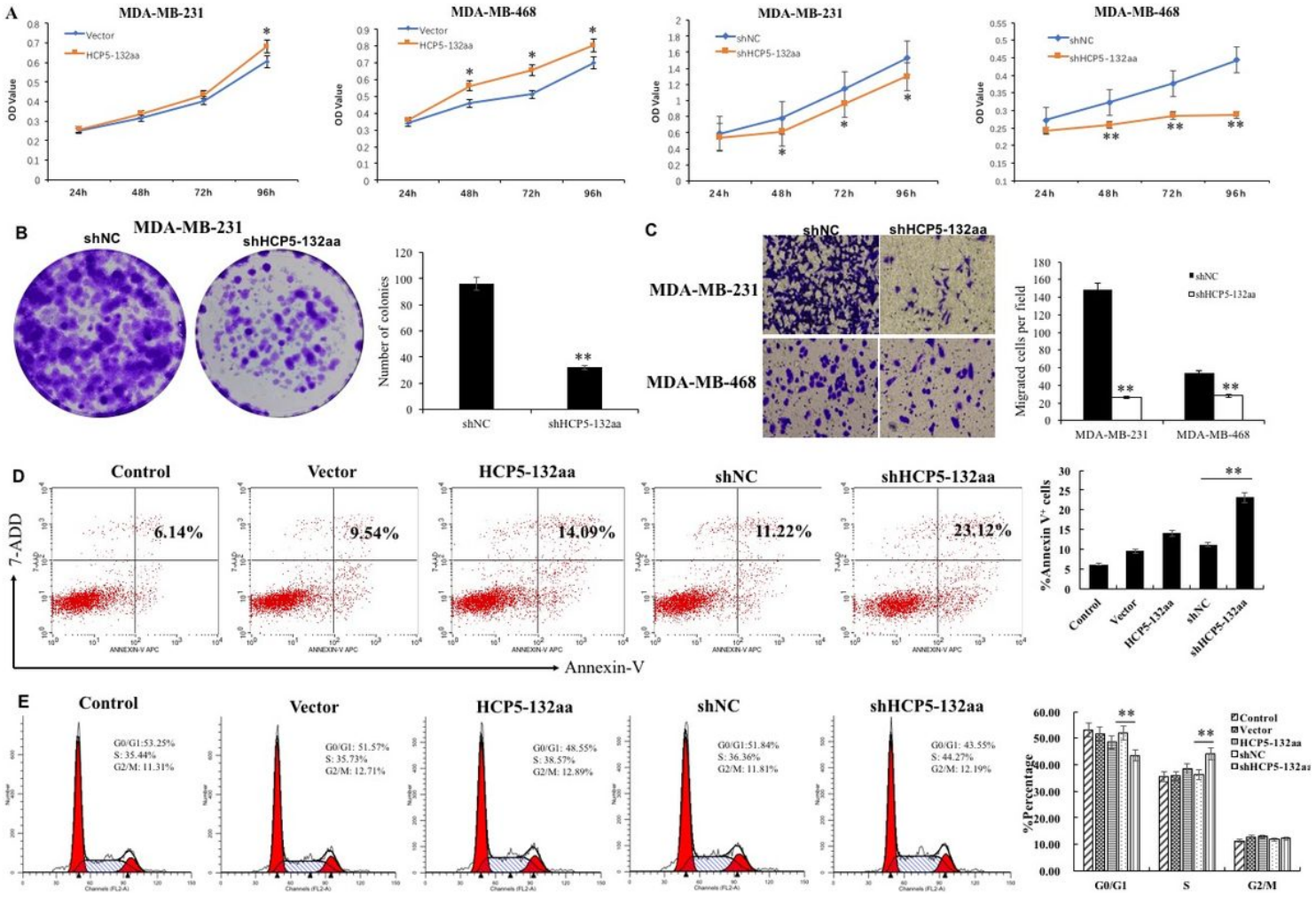

Figure 2

The HCP5-132aa promoted malignant phenotypes of TNBC cell lines. (A) MDA-MB-231 and MDA-MB-468 cells were transfected with the indicated constructs for the indicated times, and the cell numbers were measured by CCK8 (n = 3). (B) MDA-MB-231 cells were transfected with the indicated constructs, and their colony-forming abilities were measured after 2 weeks (n = 3). (C) MDA-MB-231 and MDA-MB-468 cells were transfected with the indicated constructs, and migration abilities were determined using Transwell assays (× 400). (D) MDA-MB-231 cells were transfected with the indicated constructs, and the percentage of apoptosis cellswere measured by flow cytometry. (E) MDA-MB-231 cells were transfected with the indicated constructs, and the cell cycles were measured by flow cytometry. ** P < 0.01.

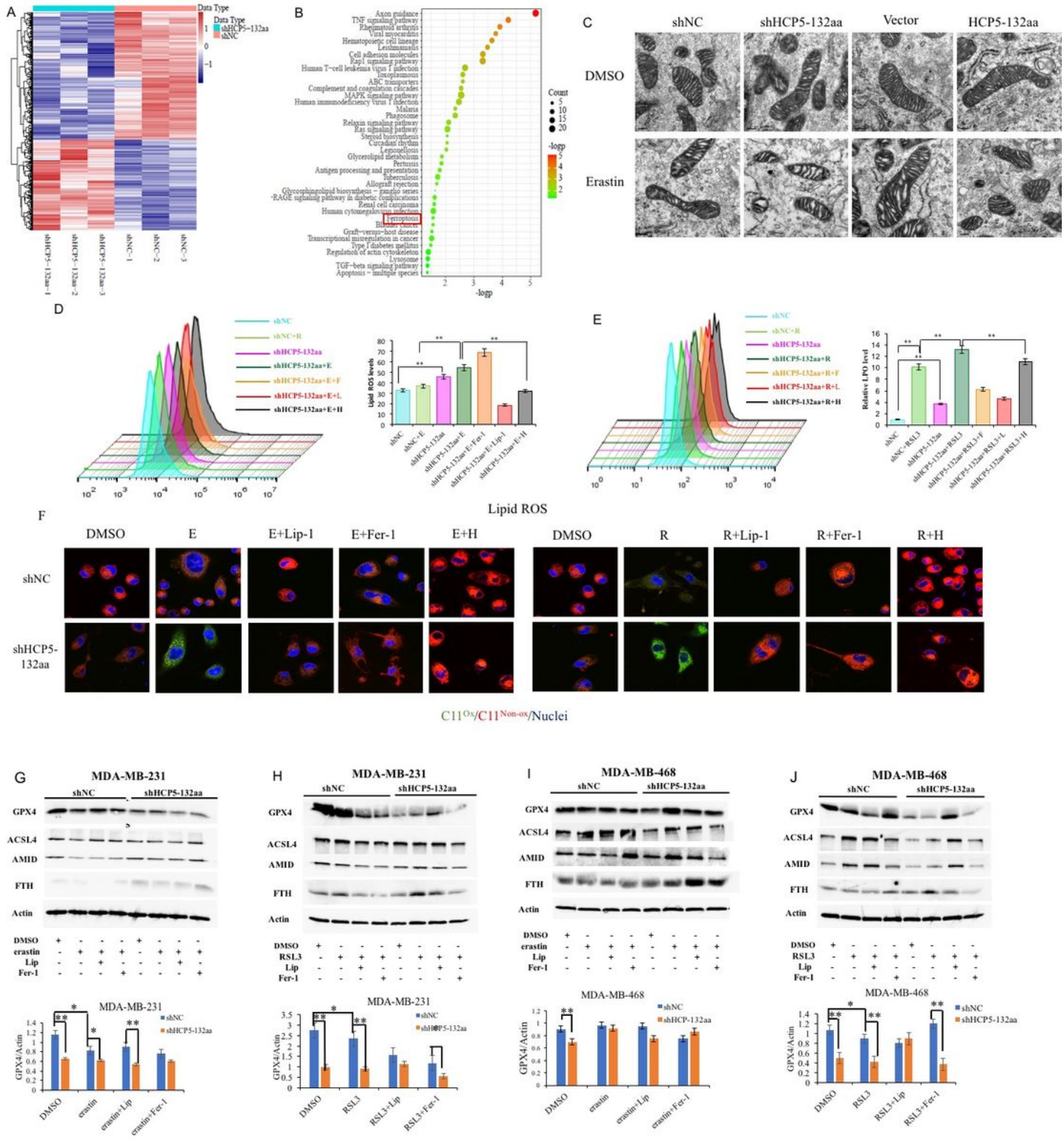

Figure 3

HCP5-132aa ORF knockdown promoted ferroptosis and synergized with ferroptosis activators. (A) The heatmap of DEGs between shHCP5-132aa and shNC MDA-MB-231 cells. (B) KEGG pathway enrichment analysis of the DEGs. (C) Mitochondrial morphological changes stimulating with Erastin in HCP5-132aa gene knockdown or overexpressed MDA-MB-231 cells were observed using transmission electron microscopy. (D-E) MDA MB 231 cells were treated with DMSO (D), Erastin (E, 15 μM), RSL3 (R, 1.25 μM),

Liproxstatin-1 (Lip-1, 50 μM), Ferrostatin-1 (Fer-1, 1 μM) or HCP5-132aa ORF overexpression plasmid (H) for 48 h, respectively. ROS generation was quantified by flow cytometry as described in the Materials and Methods section. (F) Confocal images of C11 BODIPY 581/591 in MDA-MB-231 cells. After treatment for 48 h, cells were labeled with C11 (5uM) and hoechst (1ug/mL) prior to imaging. C11Ox: oxidizedC11; C11Non-Ox: non-oxidized C11. Images are representative of two independent experiments. (G-J) HCP5-132aa ORF knockdown or negative control MDA-MB-231 and MDA-MB-468 cells were lysed after treatment with DMSO, Erastin, RSL3, Liproxstatin-1 (Lip-1) or Ferrostatin-1 (Fer-1) for 48 h. Western blot determination of ferroptosis-related proteins GPX4, ACSL4, AMID and FTH were performed. Densitometry quantification of GPX4 was normalized to actin. ** P < 0.01, * P < 0.05

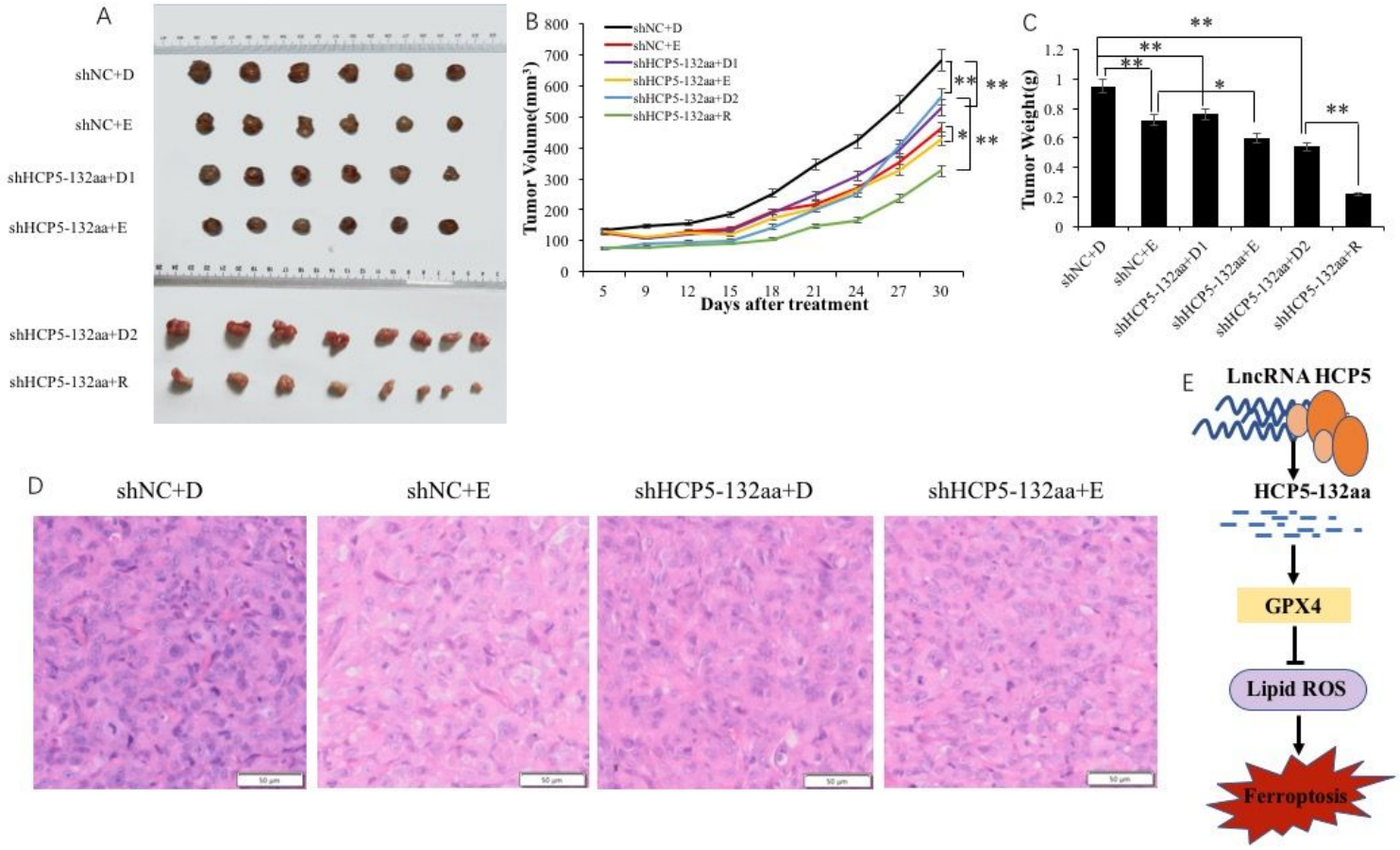

Figure 4

HCP5-132aa ORF knockdown inhibited TNBC cell growth in vivo. (A) Representative picture of tumor formation of xenograft in nude mice in shNC+DMSO, shNC+Erastin, shHCP5-132aa+DMSO, shHCP5-132aa+Erastin and shHCP5-132aa+RSL3 MDA-MB-231 cells (each group n = 6 or n = 8). (B) Summary of tumor volume and tumor weight of xenograft in nude mice. (C) Summary of tumor weight of xenograft in nude mice. (D) Representative HE stained tumor sections. (E) The schematic diagram of lncRNA HCP5 encoding protein induced cell death through ferroptosis. ** P < 0.01, * P < 0.05.

Supplementary Files

This is a list of supplementary files associated with this preprint. Click to download.

- FigureS.docx
- TableS.docx